Flat Is Not Dead: Current and Future Performance of Si-MEMS Quad Mass Gyro (QMG) System

A.A. Trusov, G. Atikyan, D.M. Rozelle, A.D. Meyer
Advanced Instrument and Sensor Development
Advanced Navigation Systems
Northrop Grumman Corporation
Woodland Hills, CA, USA

S.A. Zotov, B.R. Simon, A.M. Shkel
MicroSystems Laboratory
Mechanical and Aerospace Engineering Department
University of California, Irvine
Irvine, CA, USA

***Abstract* — This paper presents detailed performance status, modeling, and projections for the silicon MEMS Quadruple Mass Gyroscope (QMG) – a unique high Q, lumped mass, mode-symmetric Class II Coriolis Vibratory Gyroscope (CVG) with interchangeable whole angle, self-calibration, and force rebalance mechanizations. To support experimental work, a standalone CVG control and test suite was developed and implemented, comprising a packaged MEMS transducer, an analog buffer card, a digital control card, HRG-style real time closed loop control firmware, and a PC GUI for test control and data logging. Analysis of a QMG sealed without getter with a Q-factor of 1e3 reveals an Angle Random Walk (ARW) of 0.02 deg/rt-hr limited only by the fundamental Mechanical-Thermal Noise (MTN). Propagation of a detailed noise model to a QMG sealed with getter at a Q-factor of 1e6 (previously demonstrated) showed better than Navigation Grade ARW of 0.001 deg/rt-hr. Combination of the very low ARW with the mode-symmetry enabled self-calibration substantiates the navigation grade performance capacity of the Si-MEMS QMG.**

Keywords* — *Coriolis Vibratory Gyroscope, MEMS, inertial sensor, whole angle gyroscope, self-calibration, navigation grade.

I. Introduction

Coriolis Vibratory Gyroscopes (CVGs) can be divided into two classes according to the nature of the two vibration modes involved, per the IEEE STD 1431 [1]. In the Class I, the two Coriolis force coupled modes are different. The main example of MEMS Class I CVG is the dual mass Tuning Fork Gyro (TFG), such as the Draper/Honeywell MEMS gyroscope and the majority of MEMS gyroscopes in the consumer electronics and automotive application space. Higher performance MEMS Class I CVGs, typically implemented as vacuum packaged high Q-factor dual mass tuning forks, have shown reasonable Angle Random Walk (ARW) and stability in low end (Honeywell) and medium performance (Northrop Grumman LITEF) tactical grade systems.

The classic dual TFG configuration offers several attractive features such as angular gain close to the maximal theoretical value of 1, increased modal mass and drive mode amplitude, and low dissipation of energy (Q>1e5, τ>1 second), Table I. However, the technology appears to have reached its fundamental limitation with bias uncertainty on the order of 1-10 deg/hr. Reduction of bias drift by 2-3 orders of magnitude would be necessary for these devices to approach gyrocompassing and navigation grade performance, which is highly unlikely, if not fundamentally impossible, with these mature architectures.

TABLE I. Two Classes of Coriolis Vibratory Gyroscopes.

IEEE STD 1431	Class I	Class II
Modal symmetry (not axial)	✘	✓
Whole angle, self calibraiton	✘	✓
MEMS implementations	Lumpled masses	Ring, disk, shells in R&D
Angular gain, drive amplitude	✓	✘
Modal mass, time constant, Q	✓	✘
Examples	Draper/Honeywell TFG NG LITEF TFG	BAE/AIS/Goodrich/ UTC/ Silicon Sensing Vibrating Ring Gyro

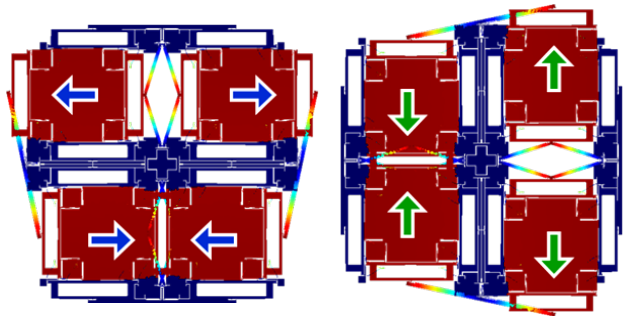

Fig. 1. Quad Mass Gyroscope resonator finite element modeling, showing the two identical mode-shapes characteristic of a Class II CVG. The QMG combines high angular gain, large drive amplitude, increased modal mass, and low dissipation advantages of MEMS tuning fork architectures with the mode-symmetry enabled stability, whole angle as well as self-calibration capabilities of Class II CVGs.

One approach to reducing the drift of Class I CVGs is to mount the MEMS IMU on a gimbaled platform, which reorients the sensors to reduce the effects of bias and scale factor uncertainties [2]. However, building a gimbaled mechanical system around a MEMS IMU significantly negates the inherent size, cost, and reliability advantages of batch

This work was supported by DARPA Micro-PNT PASCAL project N66001-12-C-4035, program manager Dr. Robert Lutwak.

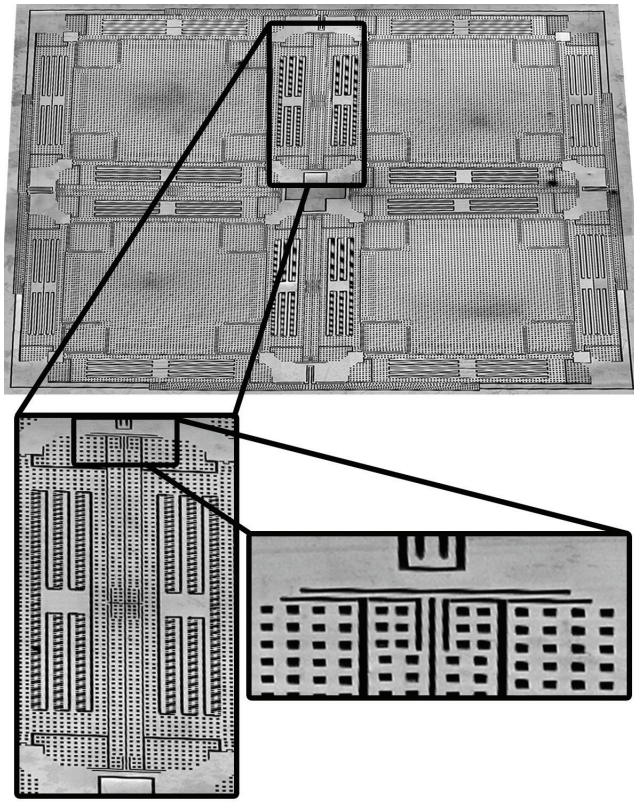

(a) SEM images illustrating the inner lever mechanism design.

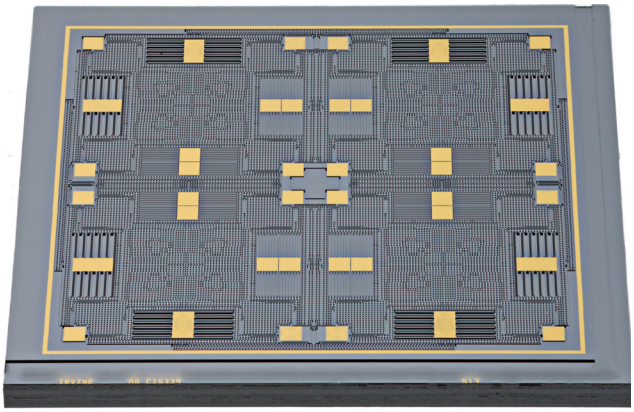

(b) Optical photograph of the gyroscope die.

Fig. 2. Batch fabricated QMG Class II CVG resonator, showing four symmetrically decoupled tines with four outer/inner lever mechanisms for anti-phase synchronization and common mode rejection [8].

micromachined solid state silicon sensors. A drastically different approach for drift reduction and performance improvement is needed, and the development of novel low dissipation Class II silicon MEMS CVGs presents such an opportunity.

In the Class II CVG, the two modes are identical, being two orthogonal degenerate modes (modes of the same natural frequency) of a symmetric elastic body. Example configurations are the vibrating string, the vibrating prismatic (square) bar, the vibrating cylindrical and hemispherical shells, vibrating rings, and in fact the Foucault pendulum [1]. Class II

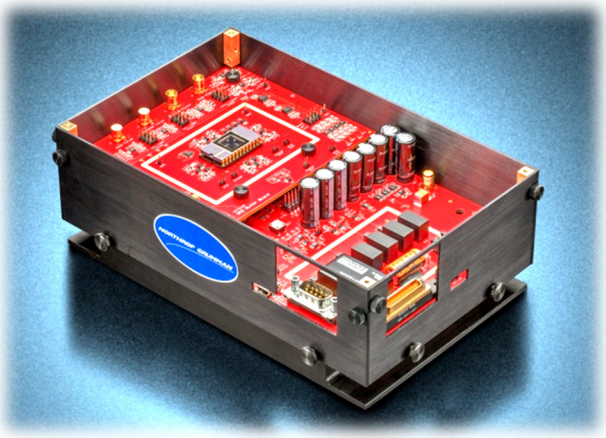

Fig. 3. Photograph of the standalone CVG controls suite fully compatible with the DARPA PALADIN test platform. The bottom card is a flexible DSP/FPGA unit; the top card has analog signal conditioning. QMG in a ceramic DIP-24 with a glass lid is in the center of the top card. The system is adaptable to other CVGs through the top card interchange.

gyroscopes can also be described as degenerate-mode, same-mode, or mode-symmetric. Unlike Class I devices, CVGs of the same-mode class can be operated in the whole-angle and self-calibration mechanizations. In the whole-angle mode, the Coriolis force resulting from input rotation is allowed to transfer energy freely between the two vibratory modes. The result (as in the Foucault pendulum) is that the change in the equivalent pendulum angle in any time interval is directly proportional to the total inertial angle the CVG has rotated through during that interval. The proportionality constant is called the angular gain, or Bryan's factor, of the CVG.

A unique enabling feature of Class II gyroscopes operated in rate measuring (or force rebalance) mode is the ability to arbitrarily place the drive-mode axis, or equivalently the pattern angle, by using proper controls. Detailed theoretical analysis predicts a change in the magnitude and polarity of the gyro bias as a function of drive axis orientation with respect to the fixed geometry of the gyro housing ("pattern angle"). By carouseling the pattern angle around the gyroscope structure, multiple error mechanisms are made observable, including frequency mismatch and misalignment, damping mismatch and misalignment, forcer and pickoff gain mismatch and misalignment, etc. Identification of these error sources through virtual carouseling (or a closely related technique called mode-reversal), enables the gyroscope system to self-calibrate bias and scale factor against device imperfections as well as variations of these imperfections throughout the lifetime of the instrument.

Mature MEMS Class II CVGs are exemplified by the BAE/ AIS/ Goodrich/ UTC and Silicon Sensing vibrating ring gyroscope. While this Class II device is potentially capable of self-calibration, its performance is limited by relatively high ARW resulting from the low modal mass, low angular gain, and insufficient ringdown time constant. These fundamental limitations of existing micromachined Class II CVGs call for a new design paradigm, which is tailored to take advantage of the inherent strength of MEMS.

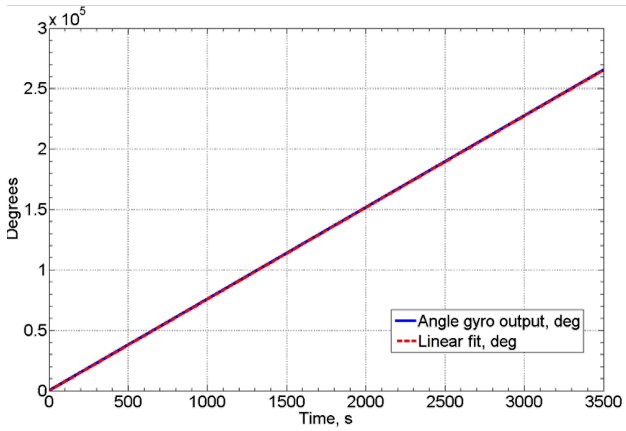

(a) Whole angle mechanization QMG output in degrees vs. time during a 100 deg/s rotation for 1 hour for a total of 0.3 million degrees.

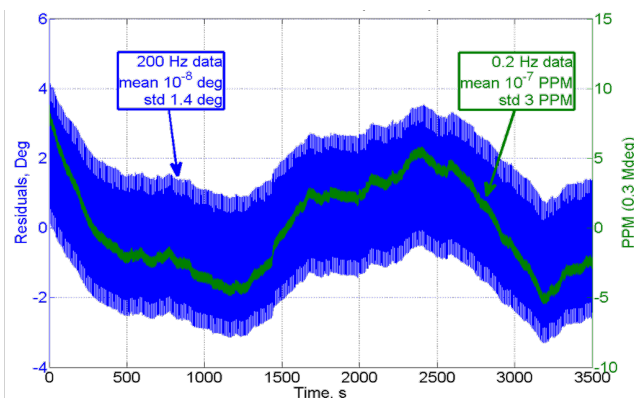

(b) Residuals of a linear fit to the angle data, showing 3 ppm stability.

Fig. 4. Whole angle demonstration using a fully closed loop QMG. The gyroscope was rotated at a 100 deg/s rate for 1 hr, showing excellent 3 ppm scale factor stability despite low Q packaging without getter.

Since MEMS geometries are defined lithographically in a single step and do not require any assembly of parts, it is beneficial to pursue the use of complex mechanical designs with multiple moving parts in order to fulfill a dream device – a low cost batch micromachined silicon MEMS Class II CVG with stiffness and damping symmetry, Q-factors above 1 million and dissipation time constants of several minutes. Quadruple Mass Gyroscope (QMG), Fig. 1, is a novel architecture [3] meeting these fundamental criteria with demonstrated low dissipation (Q>1e6 and τ>170 s when vacuum packaged with getter) and excellent modal symmetry (Δf<0.2 Hz, $\Delta(1/\tau)$<1e-4 Hz) [4,5].

This paper focuses on the performance analysis of a recently integrated fully closed loop, standalone gyro development system [6] using a QMG packaged without getter at a Q of 1e3 as well as detailed performance modeling and projections for the next generation, navigation grade system integrating a QMG transducer vacuum packaged with getter at a Q of 1e6.

II. Quadruple Mass Gyroscope Transducer

The optimal architecture of a high performance CVG comprises a mode-symmetric mechanical structure with a combination of very high Q-factor and decay time constant,

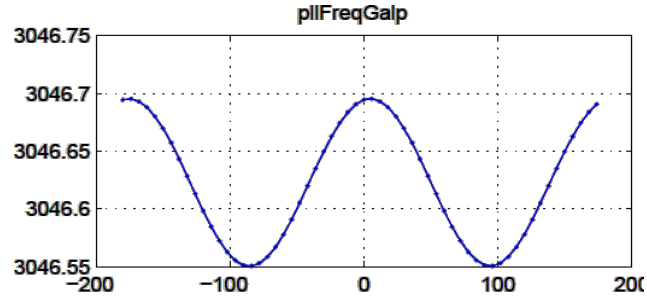

(a) Frequency in Hz vs. pattern angle in deg observing a 0.15 Hz native mismatch and nearly perfect alignment of stiffness principal axes.

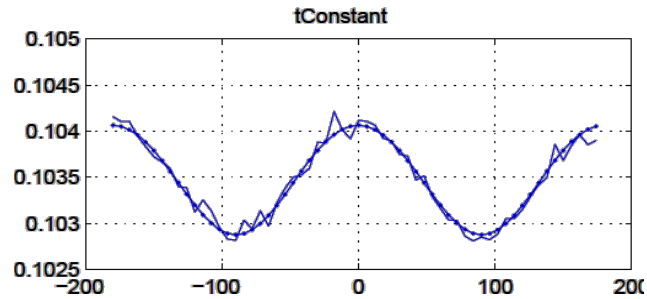

(b) Time constant τ in seconds vs. pattern angle observing a .001 second variation ($\Delta(1/\tau)$ of 0.1 Hz), and perfect alignment of principal axes.

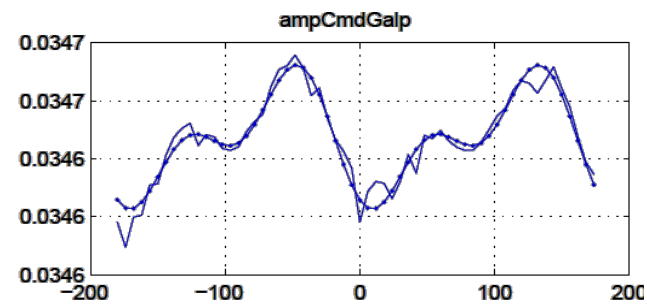

(c) Drive amplitude command (drive AC voltage amplitude) vs. pattern angle observing second and fourth harmonic variation due to the imperfections in micromachined electrostatic forcers and pickoffs.

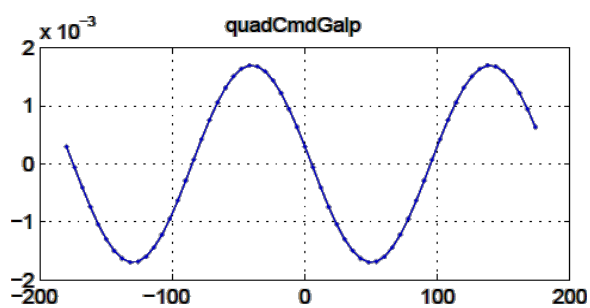

(d) Quadrature command vs. pattern angle observing a second harmonic behavior resulting from the frequency mismatch shown in subfigure (a).

Fig. 5. Demonstration of self-calibration using virtual carouseling of the Pattern Angle (PA). Mismatches and misalignments in frequency, damping, and gains are made observable as functions of pattern angle, enabling elimination of contributions to bias using D.D. Lynch models.

high Coriolis coupling (angular gain), easy frequency tuning capability [7], and low cost batch manufacturing using established silicon MEMS processes. The QMG transducer, Fig. 2, comprises four symmetrically decoupled tines

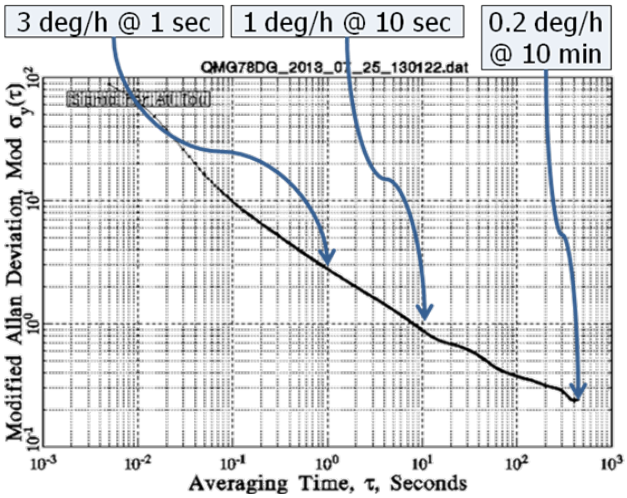

Fig. 6. Modified Allan deviation of force rebalance operated QMG sealed without getter at a Q of 1e3 showing 0.05 deg/rt-hr ARW and 0.2 deg/hr bias instability. The gyroscope full scale is 1350 deg/s, providing a dynamic range of 147 dB by virtue of digital force rebalance.

synchronized into balanced anti-phase motion by outer and inner lever mechanisms, providing a unique combination of ultra-low energy dissipation due to the elimination of anchor loss and isotropy of both the resonant frequency and damping [3-5, 6, 8]. The use of anti-phase levers instead of conventional spring flexures enables a relatively low operational frequency of several kHz, while pushing parasitic in-phase modes to higher stiffness for common mode acceleration rejection [8].

III. Standalone Gyroscope System

A fully closed loop and standalone turnkey electronics suite was developed to support experimental testing and performance analysis of the QMG, Fig. 3. The suite integrates a packaged MEMS transducer with an analog signal conditioning card and a digital control card in a single unit compatible with DARPA Platform for Acquisition, Logging, and Analysis of Devices for Inertial Navigation (PALADIN).

CVG control firmware running on the digital board implements the four primary servo loops: (1) drive amplitude, (2) drive frequency PLL, (3) sense Coriolis force rebalance, (4) sense quadrature. Additionally, the drive axis or the pattern angle can be (1) locked to a prescribed orientation for force rebalance operation, (2) allowed to precess in response to rotation for whole angle operation, or (3) commanded to slew at a prescribed rate for virtual carouseling or self-calibration.

IV. Whole Angle and Self-Calibration

A QMG with an operational frequency of 3047 Hz, as-fabricated frequency mismatch of 0.15 Hz, and a Q of 1e3 (vacuum sealed without getter) was integrated and characterized in all three mechanization modes: whole angle, self-calibration or virtual carouseling, and force rebalance rate mode. Switching between the modes is done by sending a command to the digital board through a computer GUI and does not require any hardware changes or adjustments.

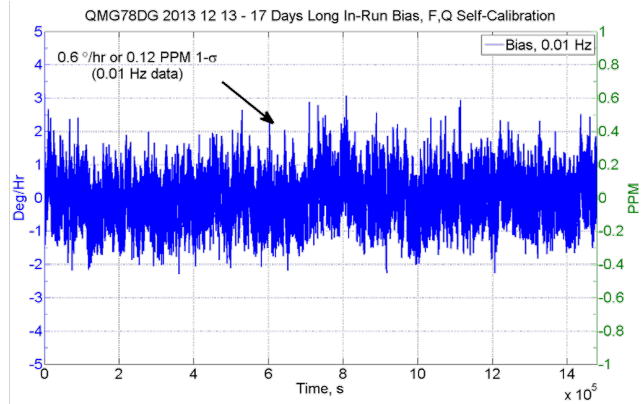

(a) Gyro bias in deg/hr and ppm of full scale vs. time in seconds. No drift is discernible in the half a month long time domain data and the standard deviation of the 0.01 Hz low pass filtered data is 0.6 deg/hr or 0.12 ppm.

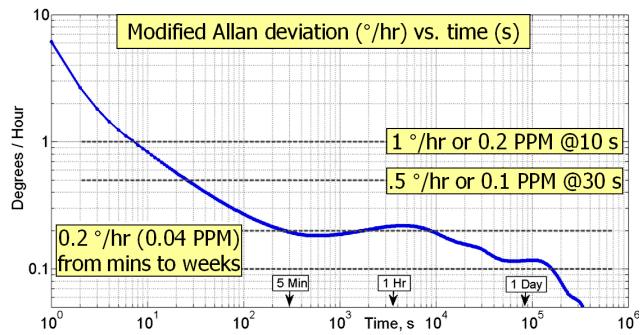

(b) Modified Allan deviation in deg/hr vs. integration time in seconds.

Fig. 7. Half a month long in-run experiment demonstrating 0.2 deg/hr stability over several weeks using a QMG transducer packaged without getter at a Q of 1e3. Self-calibration against drifts using PLL and quadrature feedback loop command signals was employed [9, 10].

To characterize operation of the whole angle mode, the gyroscope system was rotated at constant rates of ±100 deg/s for 1 hour at several different temperatures. The data, shown in Fig. 4, revealed a constant angular gain of 0.75 which agrees well with analytical modeling of the effect of the shuttle mass [4, 5]. Analysis of the linear fit to the angle data showed scale factor stability of 3 ppm, showcasing one of the inherent advantages of the whole angle mechanization of Class II CVG. It should be noted that the gyroscope is successfully operated in whole angle mechanization despite the relatively low dissipation time constant of 0.1 seconds by virtue of closed loop energy control.

Self-calibration is a closely related mechanization which uses virtual carouseling as opposed to Coriolis induced precession of the whole angle mode. Closed loop controlled intentional slewing of the pattern angle is commanded and control signals in the gyroscope servo loops are observed as functions of the pattern angle, as illustrated in Fig. 5. As a result of ±180 degrees virtual carouseling, mismatches and misalignments of stiffness and gains are identified in the nominally symmetric gyroscope. In addition, a ringdown measurement is automatically conducted at multiple equally spaced pattern angle orientations, making the damping mismatch and misalignment observable as well. The procedure

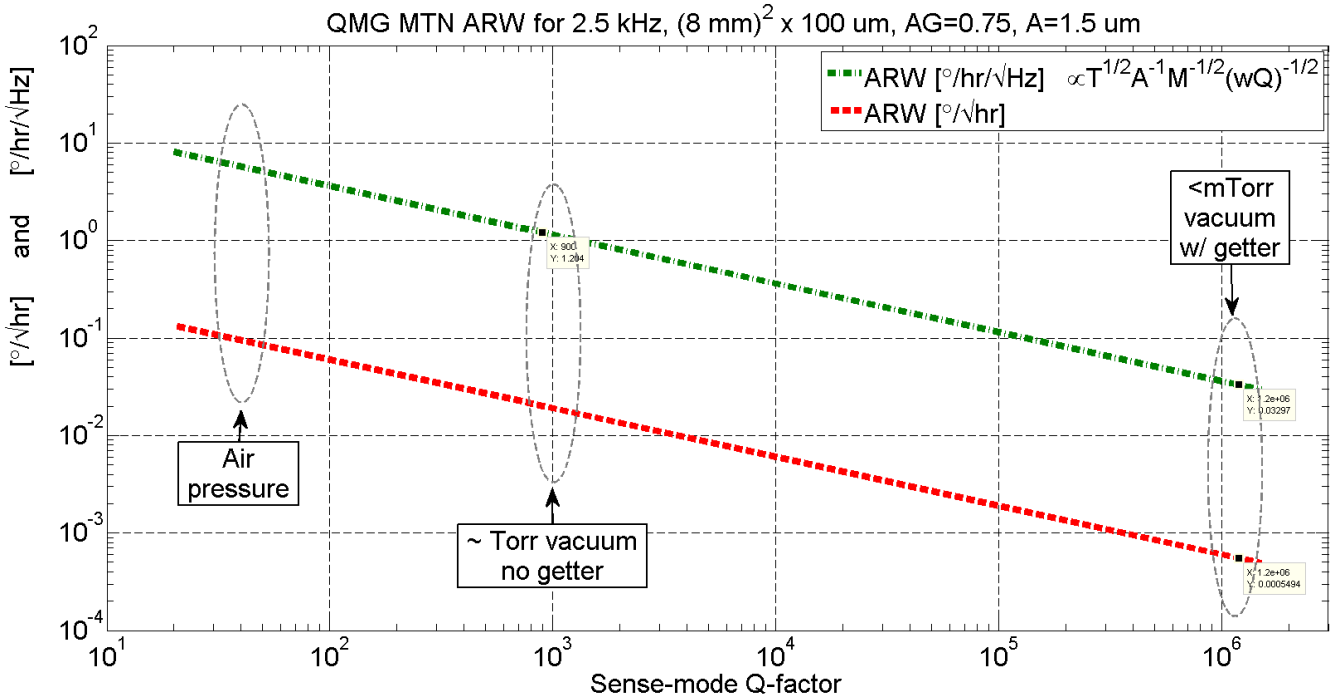

Fig. 8. Mechanical-Thermal Noise (MTN) in a QMG as a function of Q. Current QMG without getter and a Q of 1e3 is MTN limited at 1 deg/hr/rt-Hz or 0.02 deg/rt-hr, which matches with measurements. Theory predicts a 30x scaling of the ARW down to better than navigation grade 0.03 deg/hr/rt-Hz or 0.0005 deg/rt-hr for the next generation system using a QMG sealed at below 1 mTorr with getter and a Q of 1e6.

allows self identification of these individual imperfections and enables elimination of their respective bias contributions using the math models developed by D.D. Lynch for Class II CVGs such as the HRG and the QMG.

V. Force Rebalance Rate Mode

Experiments in the force rebalance rate measuring mode demonstrated a full scale of 1350 deg/s, a typical ARW of 0.02 to 0.05 deg/rt-hr, and a bias instability of 0.2 deg/hr or 0.05 ppm of the full scale, Fig. 6. Characterization over power and temperature cycles showed excellent repeatability on the order of deg/hr, currently limited by the ARW imposed measurement accuracy.

A half-month long in-run experiment was performed to assess the long term stability of the standalone gyro system, Fig. 7. Self-calibration using the PLL and quadrature feedback loop command signals was employed [9, 10]. The data demonstrates excellent stability of 0.2 deg/hr for integration times spanning from several minutes to several weeks (limited by the duration of the conducted experiment) with no discernible upward trend in the Allan deviation curve. This is attributed to the symmetry and mechanical stability of the QMG transducer as well as the advantages of digital closed loop gyro operation and self-calibration.

VI. Performance Analysis and Projections

The gyro in-run performance and the effectiveness of self-calibration against long term drifts are limited by the gyro signal-to-noise ratio or the ARW. It is thus critical to investigate the ARW governing mechanisms in the current gyro and analyze their scaling in the future QMGs vacuum packaged with getter. The best ARW measured on the tested QMG transducer packaged without getter at a Q of 1e3 was on the order of 1 deg/hr/rt-Hz or 0.02 deg/rt-hr. Mechanical-Thermal Noise (MTN) is a known fundamental noise mechanism caused by the Brownian motion of the sense-mode appearing in the gyro output as ARW [11]. While this noise source is often negligible for macroscale CVGs, it is an important consideration for MEMS devices with much smaller mass.

A detailed study of MTN scaling in the QMG as function of the quality factor and thus packaging conditions was conducted starting from the analytical formulas derived in [11] and verified and extended using direct numerical simulations of closed loop gyro dynamics with frequency mismatch imperfections under stochastic inputs. The MTN ARW for the gyroscope is

$$\frac{1}{\sqrt{4}}\frac{1}{A_G}\frac{1}{A}\sqrt{\frac{K_B T}{MQw}}\left(\frac{180}{\pi}\times 3600\right) \text{ deg/hr/rt-Hz,} \qquad (1)$$

or, equivalently,

$$\frac{1}{\sqrt{4}}\frac{1}{A_G}\frac{1}{A}\sqrt{\frac{K_B T}{MQw}}\left(\frac{180}{\pi}\times 60\right) \text{ deg/rt-hr.} \qquad (2)$$

Here, A_G=0.75 is the gyro angular gain, A=1.5e-6 m is the drive mode amplitude, M=1.7e-6 kg is the modal mass of one tine, Q=1e3 to 1e6 is the sense-mode quality factor, and w=2*pi*2.5e3 is the sense-mode resonant frequency. Additionally, the 1/√4 coefficient in front of the formulas is to account for the four statistically independent tines, T=300 K is

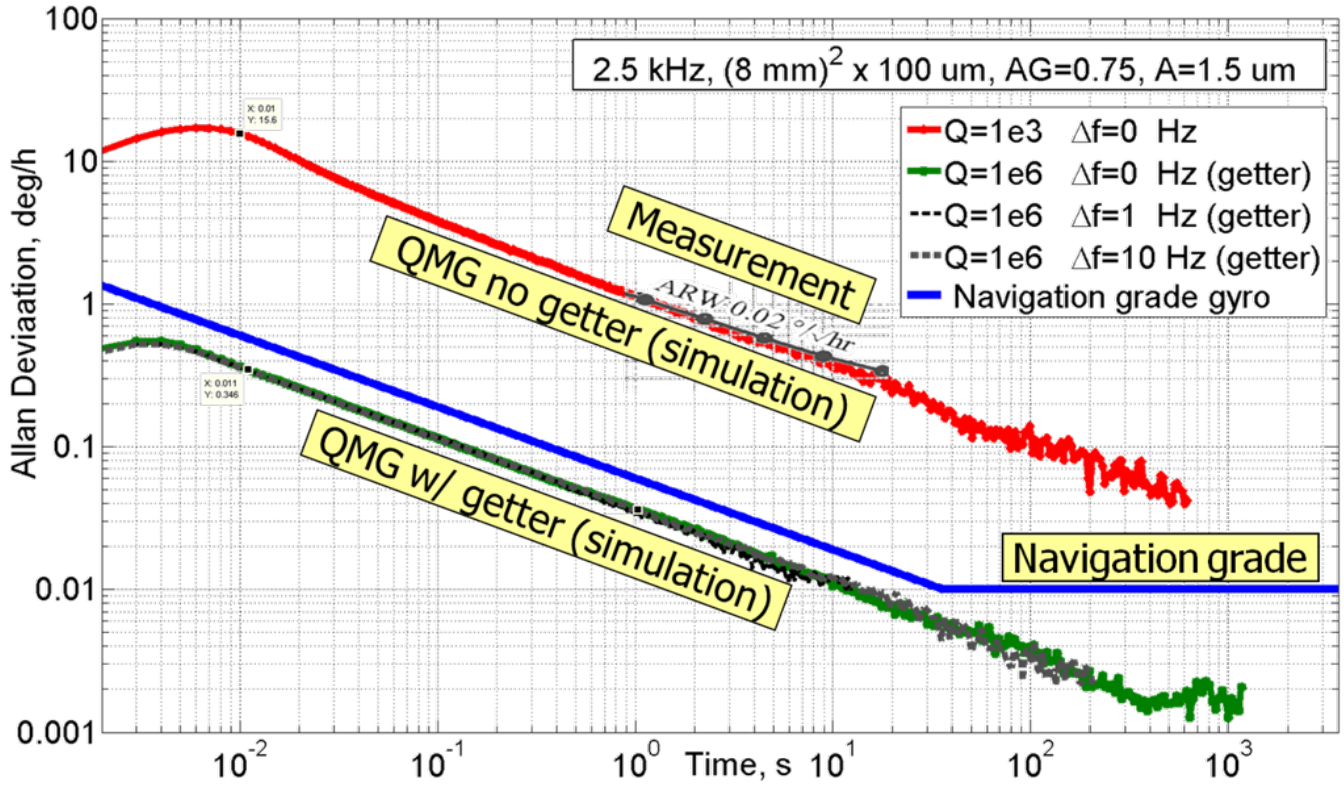

Fig. 9. Mechanical-Thermal Noise in QMG, illustrating the effects of vacuum packaging, quality factor, frequency mismatch, and closed loop operation.

the normal operating temperature, and K_B is the Boltzmann constant. Fig. 8 illustrates these formulas for the QMG for a range of quality factors from atmospheric pressure Q~50, to vacuum packaged without getter at 1 Torr and Q=1e3, to vacuum packaged with getter at 1 mTorr and Q=1e6.

Fig. 8 shows theoretical MTN ARW (1)-(2) for the baseline QMG design as a function of the Q factor and vacuum packaging conditions. When packaged without getter at a vacuum level on the order of 1 Torr and Q of 1e3 [12], the theoretical value for the fundamental MTN is 1 deg/hr/rt-Hz, which is in excellent agreement with the best measured ARW on the current QMG. This demonstrates that the current system's performance is in fact governed by the fundamental MTN mechanism and establishes the validity of MTN modeling and predictions for the future QMGs vacuum sealed with getter. Evaluation of (1)-(2) for a Q of 1.2e6, which was previously demonstrated [4, 5, 13], results in a 30 fold improvement of the ARW to 0.03 deg/hr/rt-Hz or 0.0005 deg/rt-hr, below the navigation grade ARW requirement 0.06 deg/hr/rt-Hz or 0.001 deg/rt-hr.

It should be noted that the theory [11] behind (1)-(2) and Fig. 8 assumes the case of an open loop sense-mode and perfect frequency match between the drive- and the sense-modes. This is not a feasible scenario for a high Q MEMS gyro due to the narrowing bandwidth, so it is crucial to rigorously investigate the potential effects of frequency mismatch as well as closed loop sense-mode operation on the MTN ARW. For this purpose, a detailed Simulink model was developed and tested featuring a sense-mode dynamics, Coriolis and quadrature channels, demodulation, proportional-integral rebalance loops for both the Coriolis force and quadrature channels, a rate input, and wide bandwidth stochastic MTN force input. The gains of the sense-mode feedback loops were configured to provide a gyro measurement bandwidth on the order of 100-200 Hz independent of the open loop gyro Q factor. After each simulation run, a several hour long time history of the gyro output in deg/hr at a data rate of 1 kHz was produced and analyzed using Allan deviation, Fig. 9.

The model was first executed for a QMG with a Q of 1e3 and a zero mismatch between the drive- and sense-mode frequencies. As the red curve in Fig. 9 shows, the simulation outcome of 1 deg/hr/rt-Hz ARW is indistinguishable from both the theoretical prediction of ARW using (1)-(2) in Fig. 8 as well as the best measured data, shown as gray circles. This result validates the numerical simulation approach and reconfirms MTN limited performance of the current QMG packaged without getter at a Q of 1e3.

In the following simulation runs the Q value was update to 1e6 representative of a getter packaged QMG. The frequency mismatch was set to 0 Hz, 1 Hz, and 10 Hz, shown as the green, black, and gray lines in Fig. 9. The simulation data reveals two important observations.

Firstly, the mismatch between drive- and sense-mode frequencies has no effect on MTN as long as the sense-mode dynamics is kept under Coriolis force feedback and quadrature nulling closed loop control. This allows very low noise operation of high Q MEMS gyros without requiring a perfect matching of resonant frequencies by virtue of feedback system.

Secondly, operation of the current QMG at a Q of 1e6 using getter packaging is shown to yield a navigation grade ARW of 0.03 deg/hr/rt-Hz or 0.0005 deg/rt-hr. The 30 fold improvement of the ARW has also translates into a proportional improvement in the gyro bias and scale factor self-calibration performance.

It should be noted that the quadrature nulling loop authority in the current QMG system is on the order of 10 Hz due to the large capacitance and covers the range of typical fabrication imperfections. In practice, DC voltage tuning of frequency mismatch to within 1 Hz is recommended to minimize the AC quadrature control signal coupling into the Coriolis pickoff channel caused by the phase noise of the drive waveform oscillator.

VII. Discussion on Navigation Grade MEMS

While the MTN analysis above demonstrates a clear path for the QMG to reach navigation and azimuth grade performance, it also highlights the extreme challenge of meeting these demanding requirements with MEMS technology. From (1)-(2) the following scaling laws are clear:

$$\boldsymbol{ARW_{MTN}} \propto \left(\boldsymbol{A_G} \times \boldsymbol{A} \times \boldsymbol{M} \times (\boldsymbol{Q} \times \boldsymbol{w})\right)^{-1}. \quad (3)$$

- The QMG angular gain A_G of 0.75 is close to the maximal theoretical value of 1. For comparison, the angular gain of a ring gyroscope is 0.37 for n=2 mode and just 0.17 for n=3, and can be as low as 0.01 for other high aspect ratio micromachined Class II gyros [14].
- The drive mode amplitude A of 1.5e-6 m is close to the maximum displacement on the order of 5e-6 m feasible in a MEMS device before encountering manufacturing yield issues with high aspect ratio etching as well as structural and electromechanical nonlinearities in dynamics.
- Modal mass M of 3e-6 kg achieved by using a die size of ~1 cm^2 and a thick device layer of 100 microns is close to the maximal achievable value for a low cost MEMS.
- The product of quality factor Q and frequency w. The QMG is the only silicon MEMS device that has been demonstrated to achieve thermo-elastic dissipation limited Q above 1 million and time constant of several minutes. While it may be tempting to consider improving the MTN ARW by raising the gyroscope resonant frequency, it may not be effective as the frequency times Q-factor product is limited by TED equation.

The analysis emphasizes the extreme challenge of a navigation grade capable MEMS gyroscope and outlines the attractive opportunities in further development, integration, and testing of the silicon MEMS QMG technology.

Acknowledgment

The authors thank Dr. Gunjana Sharma for assistance with MEMS fabrication, Philip R. Clark for the electronics design, James Pavell for assistance with test hardware design, and Mark R. Phillips for the computer GUI development. The MEMS gyroscope resonators were designed, fabricated, and packaged at the University of California, Irvine. The electronics design, DSP firmware and PC software development, integration, and characterization were performed at the Northrop Grumman Corporation Woodland Hills, CA campus in the Advanced Sensor and Instrument Development organization. This work was supported by DARPA Micro-PNT PASCAL project N66001-12-C-4035, program manager Dr. Robert Lutwak.

References

[1] IEEE Standard "Specification Format Guide and Test Procedure for Coriolis Vibratory Gyros," IEEE Std 1431-2004 , vol., no., pp.1,78, Dec. 20 2004.

[2] J.E. Pritchet, C. Lange, J. Warren, "System Design Trades in Gimballed MEMS Northfinding Systems," ION JNC 2012.

[3] A.A. Trusov, A.R. Schofield, A.M. Shkel, "Micromachined Tuning Fork Gyroscopes with Ultra-High Sensitivity and Shock Rejection," US Patent 8,322,213.

[4] A.A. Trusov, I.P. Prikhodko, S.A. Zotov, A.M. Shkel, "Low-Dissipation Silicon MEMS Tuning Fork Gyroscopes for Rate and Whole Angle Measurements," IEEE Sensors J., vol. 11, no. 11, pp. 2763-2770, Nov. 2011.

[5] I.P. Prikhodko, S.A. Zotov, A.A. Trusov, A.M. Shkel, "Sub-Degree-per-Hour Silicon MEMS Rate Sensor with 1 Million Q-Factor," Transducers 2011.

[6] A.A. Trusov, D.M. Rozelle, G. Atikyan, B.R. Simon, S.A. Zotov, A.M. Shkel, A.D. Meyer, "Force Rebalance, Whole Angle, and Self-Calibration Mechanization of Silicon MEMS Quad Mass Gyro," IEEE ISISS 2014.

[7] K. Shcheglov, "DRG - a High Performance MEMS Gyro," Joint Precision Azimuth Sensing Symposium 2010.

[8] B.R. Simon, A.A. Trusov, A.M. Shkel, "Anti-Phase Mode Isolation in Tuning-Fork MEMS Using a Lever Coupling Design," IEEE Sensors 2012.

[9] D.M. Rozelle, "The Hemispherical Resonator Gyro: From Wineglass to the Planets," 19th AAS/AIAA Space Flight Mechanics Meeting 2009.

[10] S.A. Zotov, B.R. Simon, G. Sharma, A.A. Trusov, A.M. Shkel, "Utilization of Mechanical Quadrature in Si-MEMS Gyro to Increase and Expand Long Term In-Run Bias Stability," IEEE ISISS 2014.

[11] R. Leland, "Mechanical-thermal noise in MEMS gyroscopes," IEEE Sensors J., vol. 5, no. 3, pp. 493–500, Jun. 2005.

[12] I.P. Prikhodko, B.R. Simon, G. Sharma, A.A. Trusov, A.M. Shkel, "High and Moderate Level Vacuum Packaging of Vibratory MEMS," IMAPS 2013, Orlando, FL, USA, Sept. 30 – Oct. 3, 2013.

[13] S.A. Zotov, A.A. Trusov, A.M. Shkel, "High-Range Angular Rate Sensor Based on Mechanical Frequency Modulation," IEEE/ASME JMEMS, vol. 21, no. 2, pp. 398-405, April 2012.

[14] J. Cho, J.A. Gregory, K. Najafi, "High-Q, 3kHz Single-Crystal-Silicon Cylindrical Rate-Integrating Gyro (CING)," IEEE MEMS 2012.